ENVIRONMENTAL RESEARCH
LETTERS

LETTER • OPEN ACCESS

More than a nuisance: measuring how sea level rise delays commuters in Miami, FL

To cite this article: Mathew Hauer *et al* 2021 *Environ. Res. Lett.* **16** 064041

ENVIRONMENTAL RESEARCH
LETTERS

LETTER

More than a nuisance: measuring how sea level rise delays commuters in Miami, FL

Mathew Hauer[1,2], Valerie Mueller[3,4], Glenn Sheriff[3,*] and Qing Zhong[5]

[1] Department of Sociology, Florida State University, 600W. College Ave., Tallahassee, FL 32306
[2] Center for Demography and Population Health, Florida State University
[3] School of Politics and Global Studies, Arizona State University, PO Box 873902, Tempe, AZ 85297-3902
[4] International Food Policy Research Institute, 1201 Eye St., NW, Washington, DC 20005-3915
[5] School of Geographical Sciences, Nanjing University of Information Science and Technology, Nanjing, People's Republic of China
[*] Author to whom any correspondence should be addressed.

E-mail: gsheriff@asu.edu

OPEN ACCESS

RECEIVED
19 November 2020

REVISED
23 April 2021

ACCEPTED FOR PUBLICATION
30 April 2021

PUBLISHED
26 May 2021

Keywords: sea level rise, climate accommodation, commute times, transportation, tidal flooding, Miami

Supplementary material for this article is available online

Abstract

Sea level rise increases coastal cities' exposure to tidal flooding and elevates the risk of transportation routes being compromised at high tide. Using Miami, Florida as a case study, we combine tide gauge, elevation, road network, and worker location data with a route optimization algorithm to model how tidal flooding affected commute times between 2002–2004 and 2015–2017. Results suggest tidal flooding increases annual commutes by 15 min on average and 274 min among the most heavily impacted areas. Additionally, approximately 14 000 commuters may be unable to reach their workplace due to tidal flooding at least once per year. Accommodation via dynamic adjustments in residential and work locations may reduce tidal commuting delays by as much as 70%, particularly among the highest earners. Many of the most affected areas do not experience flooding directly, expanding the purview of vulnerability beyond simple residential risk. Using 2060 extreme sea-level rise scenarios without accommodating behavior, mean annual commute delays are expected to reach 220 min with over 55 000 commuters potentially unable to reach their destinations.

1. Introduction

Sea level rise (SLR)-induced flooding poses a threat to the economic vitality of coastal cities (Hallegatte *et al* 2011, Clark *et al* 2016, Garner *et al* 2017, Hsiang and Kopp 2018, Kopp *et al* 2019, Kocornik-Mina *et al* 2020, Desmet *et al* 2021). Considerable research has examined the direct impact of local exposure to hurricanes, storm surges, and flooding on real estate (Carbone *et al* 2006, Michael 2007, Bin and Landry 2013, Hinkel *et al* 2014, Deryugina *et al* 2018, Bakkensen *et al* 2019, Bernstein *et al* 2019, Yi and Choi 2019). Apart from permanent flooding and extreme events, SLR is expected to increase the extent of tidal ('sunny day' or 'nuisance') flooding (Moftakhari *et al* 2015, Dahl *et al* 2017, Sweet *et al* 2018). An emerging literature has begun to investigate the impacts of this less dramatic but more frequent type of flooding on property (Moftakhari *et al* 2017, McAlpine and Porter 2018, Bukvic and Harrald 2019), transportation (Jacobs *et al* 2018, Kasmalkar *et al* 2020, Shen and Kim 2020, Praharaj *et al* 2021), and economic activity (Hino *et al* 2019).

We extend this research by modeling recent commuting delays, relative to hypothetical 'dry' conditions, attributable to tidal flooding for the Miami metropolitan area, how this burden has changed over the last 15 years, and how it could change with 2060 SLR projections. This focus differentiates our study from the bulk of the transportation literature which measures various location vulnerability (or accessibility) metrics. Instead, our work is most closely related to the Jacobs *et al* (2018) analysis of the U.S. eastern coast and the Kasmalkar *et al* (2020) study of the San Francisco area, combining elements of each.

As in Jacobs *et al* (2018), we employ historical and projected tide gauge readings to estimate a distribution of daily flooding impacts for each road segment.

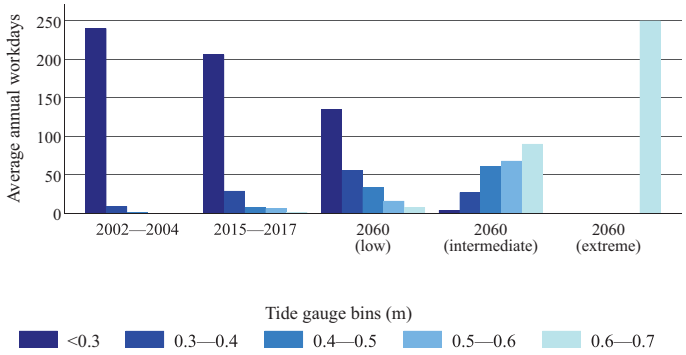

Figure 1. Tide bins and average annual number of normalized workdays for which maximum tide gauge reading is in each bin. Source: author calculations based on historic NOAA data and intermediate SLR scenario from NOAA projections (Sweet *et al* 2017).

Like Kasmalkar *et al* (2020), we (a) relax the assumption that roads are either unaffected or impassable, allowing passage on partially flooded road segments at reduced speed, (b) use data on commuter origin and destination rather than average annual road use, and (c) use an optimization algorithm to determine the fastest route between home and work conditional on road conditions. This combined approach allows us to estimate delays based on empirical tide readings while allowing for behavioral change in any given year.

We take the above approach a step further, decomposing the changing impact of SLR over time into a 'tide effect' and 'accommodation'. The tide effect captures delays attributable purely to changes in tidal flooding over the two periods, assuming commuters retain their first-period home and work locations. As opposed to retreat or protection, accommodation refers to a form of adaptation in which people change how they use land at increased risk of flooding (Dronkers *et al* 1990). Specifically, here it reflects the aggregate impact on second-period delays arising as commuters change home and work locations from those in period one. The decomposition provides an indicator of the importance of long-term behavioral changes useful for considering benefits of future adaptive infrastructure investments (Adger *et al* 2009, Hauer 2017). Commuter income data allow us to explore connections between earnings and capacity for accommodation. Although our results are consistent with accommodating behavior among all income levels, they suggest that highest-earning commuters may be those most able to mitigate the impacts of flooding on commuting times.

Looking forward, we use the most recent 2060 low, intermediate, and extreme SLR scenarios published by the National Oceanographic and Atmospheric Administration (NOAA) (Sweet *et al* 2017) to project how the tide effect is likely to evolve over time. By considering the number of days each year that each road is likely to experience a given level of tidal flooding, these projections provide a more nuanced understanding of these impacts relative to studies that rely on changes in 100-year floodplains (Suarez *et al* 2005) or isolated flooding scenarios (Sadler *et al* 2017, Kasmalkar *et al* 2020).

Our case study concentrates on the Miami metropolitan area, home to a quarter of the SLR-exposed U.S. population (Hauer *et al* 2016). Figure 1 shows tide levels above 0.3 m in elevation were infrequent (10 d) as recently as 2002–2004 but increased over four-fold (44 d) in 2015–2017. With limited offerings of public transportation (Florida and Pedigo 2019), these private SLR costs are borne by those commuting by car. Thus, our estimates can contribute to a greater understanding of the benefits of implementing adaptation policies (in terms of the value of recuperating the time lost to commuting delays) as flooding events become commonplace in 2060 (Kulp and Strauss 2017).

2. Methods

To reduce potential influence of an anomalous year, our primary results evaluate commuting delays comparing changes in tide levels over two historical three-year periods: 2002–2004 (Period 1) and 2015–2017 (Period 2). These two periods do not take place at the same point in lunar nodal and perigean cycles. Consequently, this analysis is best interpreted as measuring the effects of a change in tides between these periods resulting from the combined impact of SLR-driven flooding and lunar cycle-driven flooding. We also predict commuting delays for 2060 (Period 3) based on projected tide gauge readings corresponding to NOAA's low (0.19 m), intermediate (0.45 m), and extreme (0.9 m) SLR scenarios (Sweet *et al* 2017).

Calculation of mean regional commuting delays proceeds in six steps. We first obtain the range of tide gauge readings for each period. We then model road inundation depth as a function of a given tide gauge reading. In a third step, we model travel velocity

for each road segment as a function of inundation. Fourth, we select the fastest route between any two points, conditional on this velocity. Next, we use the observed distribution of tidal gauge readings in each period to calculate the average annual flooding delay for a given pair of points. Finally, we obtain aggregate commuting delays for the Miami area by taking the weighted average annual delay over all home-work location pairs, where the weights correspond to the number of commuters travelling from a given home location to a work location in the period. We detail each of these steps below.

2.1. Step 1: tide gauge readings

We collect data on maximum hourly gauge readings recorded for each weekday (Monday-Friday) between the hours of 05:00 and 20:00. For Periods 1 and 2, readings for the Virginia Key, Biscayne Bay, FL tide gauge—the most centrally located tide gauge in our study area—come from the NOAA Center for Operational Oceanographic Products and Services database. We download hourly verified high/low water levels for the period 2002–2017 using the 'rnoaa' package (Chamberlain 2019), implemented in the R programming language. To correct for extreme values corresponding to hurricanes, we deploy an outlier detection algorithm (Chen and Liu 1993, de Lacalle 2019) to search and correct for extreme outliers in the time series and generate a counterfactual tide gauge time series. We use the counterfactual value in time periods in which the observed gauge exceeds a critical threshold (τ or t-statistic). This procedure identified two days with extreme water heights ($\tau \geqslant 10$; 24.10.2005 and 10.09.2017) corresponding to hurricanes Wilma and Irma. To project anticipated tide gauge values in Period 3, we add the change in NOAA SLR scenario values from 2017 to 2060 in Sweet *et al* (2017) to Period 2 daily tide values.

For computational tractability, we group the tide gauge readings into five discrete bins. Figure 1 displays the number of days falling in each bin for each period and SLR scenario. For each period and scenario, there is a vector $\mathbf{g} = (g_1, g_2, \ldots, g_5)$ with typical element g_b being the mean workday high gauge reading for bin b. Table S1 (available online at stacks.iop.org/ERL/16/064041/mmedia) presents the values of $\mathbf{g}$.

2.2. Step 2: local inundation as a function of road elevation and tide gauge

We obtain surface elevation for each road segment by merging the 2019 road network, extracted from Miami-Dade County (2020) and U.S. Census Bureau (2020a), with the 1/9 arc-s (10 m) National Elevation Dataset (Gesch *et al* 2002). Applying a 'bathtub' hydrological model, similar to that used by NOAA for mapping tidal flooding (NOAA 2017), we calculate road segment inundation levels as the difference between the water levels reported at the tide gauge and road surface elevation. While not perfect, a single-cell bathtub model provides a useful representation of subsurface flows given the region's porous limestone geology. Figure 2 displays areas of the two counties (not just roadways) subject to flooding at each tide gauge level.

For further tractability, we discretize mm of inundation into five bins (0, 0–100, 100–200, 200–300, >300). For any given road segment the variable $i(g_b)$ represents the midpoint value of the bin corresponding to the modeled inundation depth as a function of the tide gauge reading.

2.3. Step 3: travel velocity as a function of local inundation

Statutory speed limits for major roads and bridges come from the Florida Department of Transportation (Florida Department of Transportation 2020b). We assume the speed limit of all other roads to be 25 mph (Florida Department of Transportation 2020a). To incorporate the influence of flooding, we model travel velocity v in mph as a function of the speed limit L and mm of road inundation i:

$$v(i(g_b)) = \begin{cases} L & i(g_b) = 0 \\ \min\left\{L, 0.6[0.0009 i(g_b)^2 - 0.5529 i(g_b) + 86.9448]\right\} & 0 < i(g_b) < 300 \\ 1 & 300 \leq i(g_b). \end{cases} \quad (1)$$

We base this model on the depth-disruption function fitted by Pregnolato *et al* (2017). Besides making inundation a function of the tide gauge, we modify their function in three key aspects: (a) with no flooding we assume vehicle speed to be the statutory limit; (b) with flooding less than 300 mm we assume vehicle speed to be the minimum of the statutory limit or the maximum safe speed estimated by Pregnolato *et al* (2017); and (c) our main analysis assumes a maximum safe speed of one mph, rather than zero, after inundation reaches 300 mm (the average depth at which passenger vehicles start to float, see Pregnolato *et al* (2017)). Under an alternate assumption that 300 mm of inundation renders these segments impassable, our secondary analysis calculates the

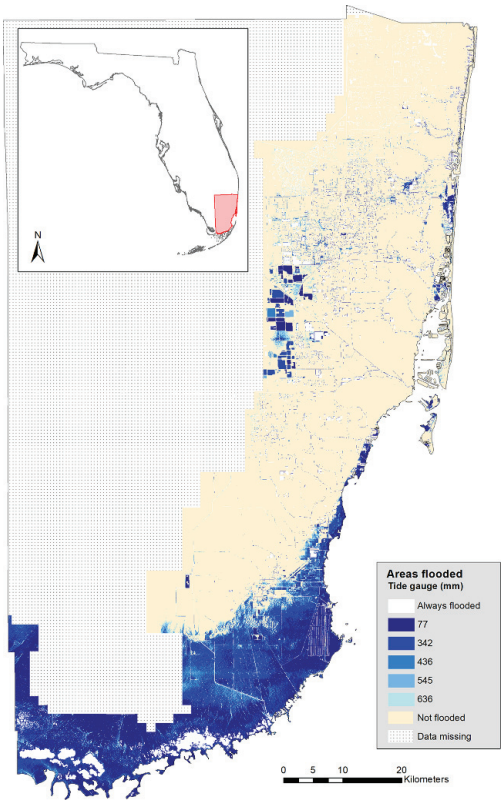

Figure 2. Tidal flooding, Miami-Dade and Broward Counties. Colors depict locations that become flooded as the tide gauge reaches the indicated level. Darkest blue, for example, represents low-lying areas such as canals and marshes that are flooded at a tide gauge reading of 77 mm, while the next lighter shade is areas of higher elevation that become flooded at a 342 mm tide gauge. Source: author calculations based on Gesch *et al* (2002).

number of commuters who are unable to reach their destinations.

2.4. Step 4: calculating optimal travel times

The next step identifies the fastest route between each origin (home) and destination (work) location conditional on the tide gauge reading. We generally assume the precise origin and destination points to be Census Block Group (CBG) population centroids. The CBG is the smallest geography at which the U.S. Census publishes sample data. Boundaries are typically streets, bodies of water, or legal jurisdictions, and do not cross county lines. CBGs generally have between 600 and 3000 residents. If the work CBG centroid does not lie within the U.S. Census-defined Miami urbanized area we use the centroid of the portion of the work CBG in the urbanized area. Unless indicated otherwise in the extracted road data, we assume all segments to be bi-directional and to connect to crossing road segments. Under these assumptions, we use the ArcGIS Network Analyst algorithm to obtain the minimum travel time between each home and work CBG pair conditional on the tide gauge. The 'dry' travel time between CBG pairs ranges from less than a minute to about one hour and 45 min, with a mean of approximately 25 min.

2.5. Step 5: average annual flooding delays for each home-work pair

Each year has a different number of recorded weekdays. To aggregate across three-year periods we normalize each year into 250 workdays, using the proportion of observed weekdays in each tide gauge bin. Letting d_{by} denote the number of workdays in tide bin b in year y, we compute the annual average number of normalized weekdays in bin b in a three-year period (with y indexing years) as:

$$d_b = \frac{1}{3}\sum_{y=1}^{3} \frac{d_{by}}{\sum_{b=1}^{5} d_{by}} \times 250. \qquad (2)$$

Let H and W be the total number of home and work CBGs, indexed by h, and w. Optimal minutes of travel time as a function of tide gauge bin values g_b (listed in table S1) is $m_{hw}(g_b)$. For a vector $\mathbf{d} = (d_1, d_2, \ldots, d_5)$ of days in each tide bin, the annual round-trip tidal flooding delay (in min) for a commuter on a given home-work pair hw is:

$$c_{hw}(\mathbf{d}) = 2\sum_{b=1}^{5} \left[m_{hw}(g_b) - m_{hw}(\underline{g})\right] d_b; \qquad (3)$$
$$h = 1, 2, \ldots, H; w = 1, 2, \ldots, W.$$

Here, $\underline{g}$ denotes the maximum tide gauge value for which inundation depth is zero for all road segments, i.e. $m_{hw}(\underline{g})$ is the 'dry' travel time for each pair.

2.6. Step 6: aggregating flooding delays across the Miami area

We obtain annual commuting trips from the U.S. Census Bureau's Longitudinal Employer-Household Dynamics Origin-Destination Employment Statistics (LODES) for the period 2002–2017 (U.S. Census Bureau 2020b). LODES is a partially synthetic dataset containing CBG-level information of paired home and work locations with comprehensive coverage across the United States. LODES reports data for about 2530 CBGs in Miami-Dade and Broward counties, for a total of over 2.8 million home-work combinations. LODES disaggregates commuters into three income categories: less than $1250 per month, between $1251 and $3333 per month, and over $3333 per month. In Period 2, the number of commuters in a home-work CBG pair ranged from 0 to 1097, with an average of 1.7 for all pairs in Miami-Dade and Broward counties.

To calculate the average regional commuting delay in a given period we use LODES to generate a vector $\mathbf{p} = (p_{11}, p_{12}, \ldots, p_{hw}, \ldots, p_{HW})$ for the whole sample and for each income category. Each element represents the number of people residing in CBG h who commute to CBG w. Period 3 analysis uses the $\mathbf{p}$ vector corresponding to Period 2.

The aggregate outgoing commuting delays caused by flooding for a home CBG is the sum over all work CBGs, weighted by the number of commuters in the income category:

$$c_h(\mathbf{d},\mathbf{p}) = \sum_{w=1}^{W} c_{hw}(\mathbf{d})p_{hw}; \text{for all } h = 1,2,\ldots,H. \quad (4)$$

Similarly, $c_w(\mathbf{d},\mathbf{p})$ represents the aggregate incoming commuting delays from all home CBGs to a given work CBG,

$$c_w(\mathbf{d},\mathbf{p}) = \sum_{h=1}^{H} c_{hw}(\mathbf{d})p_{hw}; \text{for all } w = 1,2,\ldots,W. \quad (5)$$

For each income category, the total annual commuting delay for the Miami area over a given three year period is then

$$C(\mathbf{d},\mathbf{p}) = \sum_{h=1}^{H} c_h(\mathbf{d},\mathbf{p}) = \sum_{w=1}^{W} c_w(\mathbf{d},\mathbf{p}). \quad (6)$$

These calculations do not include people whose home and work are in the same CBG or whose home or work CBG is outside Miami-Dade and Broward counties.

We evaluate flooding impacts for three categories of home-work pairs: all 2.8 million pairs in Miami-Dade and Broward counties, the 495 thousand pairs affected by flooding in Period 2, and the 160 thousand pairs above the 95th percentile of commuting delays in Period 2.

Two factors cause commuting delays to change across time periods, a change in the vector $\mathbf{d}$ of days in each tide bin, and a change in the vector $\mathbf{p}$ of people utilizing each home-work pair. We exploit these two sources of change to decompose the total change in commuting delays between two periods into a 'tide effect' and 'accommodation.' Letting superscripts denote periods,

$$\underbrace{C(\mathbf{d}^2,\mathbf{p}^2) - C(\mathbf{d}^1,\mathbf{p}^1)}_{\text{total change}} = \underbrace{C(\mathbf{d}^2,\mathbf{p}^1) - C(\mathbf{d}^1,\mathbf{p}^1)}_{\text{tide effect}} + \underbrace{C(\mathbf{d}^2,\mathbf{p}^2) - C(\mathbf{d}^2,\mathbf{p}^1)}_{\text{accommodation}}. \quad (7)$$

The tide effect indicates the change in commuting delays that would occur if the number of days in each tide bin changed, but the number of commuters in each home-work pair remained constant at Period 1 levels. The accommodation effect reflects how the change in commuter choice of home and work locations affected delays holding the number of days in each bin constant for Period 2.

Changes in the number of commuters in each home-work pair can theoretically reflect adaptive changes in behavior to lessen the impacts of flood exposure *all else equal*. Since our model uses the same road network for each period, these figures do not incorporate adaptation in the physical infrastructure itself. We do not claim to identify a causal relationship between changes in flooding and changes in commuting patterns since we do not observe commuting changes that might have occurred in the absence of SLR or over similar nodal and perigean cycles. Instead, this accommodation is best interpreted as the impact on commuting times of changes in behavior over time, regardless of motivation. We use these two metrics to explore the extent to which accommodation offsets flood-driven increases in commuter delays.

3. Results

We evaluate the tidal flooding impact on commuters in three periods, Period 1 (2002–2004), Period 2 (2015–2017), and Period 3 (2060). Our unit of analysis is the pair of CBG centroids describing a potential worker's home and work locations. We evaluate flooding impacts for three categories of home-work pairs: all 2.8 million pairs in Miami-Dade and Broward counties, the 495 thousand pairs affected by flooding in Period 2, and the 160 thousand pairs above the 95th percentile of flooding costs in Period 2. Our main analysis assumes road segments flooded at a depth exceeding 30 cm are passable at a speed of 1 mph. Our secondary analysis instead assumes these segments are impassable, calculating the number of commuters who are unable to reach their destination.

We initially describe the commuting delays experienced in Period 2 (2015–2017), assuming all road segments passable. The model suggests that tidal flooding added 15.44 min year^{-1} to the average commuter's travel time in Miami-Dade and Broward counties spread over the entire commuting population (table 1 and figure 3). Conditional on being impacted at all, the average annual delay was considerably higher—103.38 min—with the 95th percentile average commuting delay of more than 4.5 h year^{-1}. These burdens are 1.43 min, 5.99 min, and 8.21 min more than Period 1, suggesting a detectable, increasing commuting burden. Figure 3(a) displays how commuting delays are distributed across the population. For Periods 1 and 2, despite the modest changes in mean commuting times, the upper tails of the distributions in later years thicken, indicating growth in the proportion of commuters facing substantial flooding impacts.

Under the alternative assumption that road segments are impassable at a depth of 30 cm, travel between some home-work pairs becomes infeasible once the tide gauge reaches a certain point, i.e. there are *no* routes that connect these pairs without traversing a water depth greater than 30 cm. Using this assumption our secondary analysis finds that 0.84% of the entire commuter population, 5.64% of those with any commuting impact, and 7.82% of the

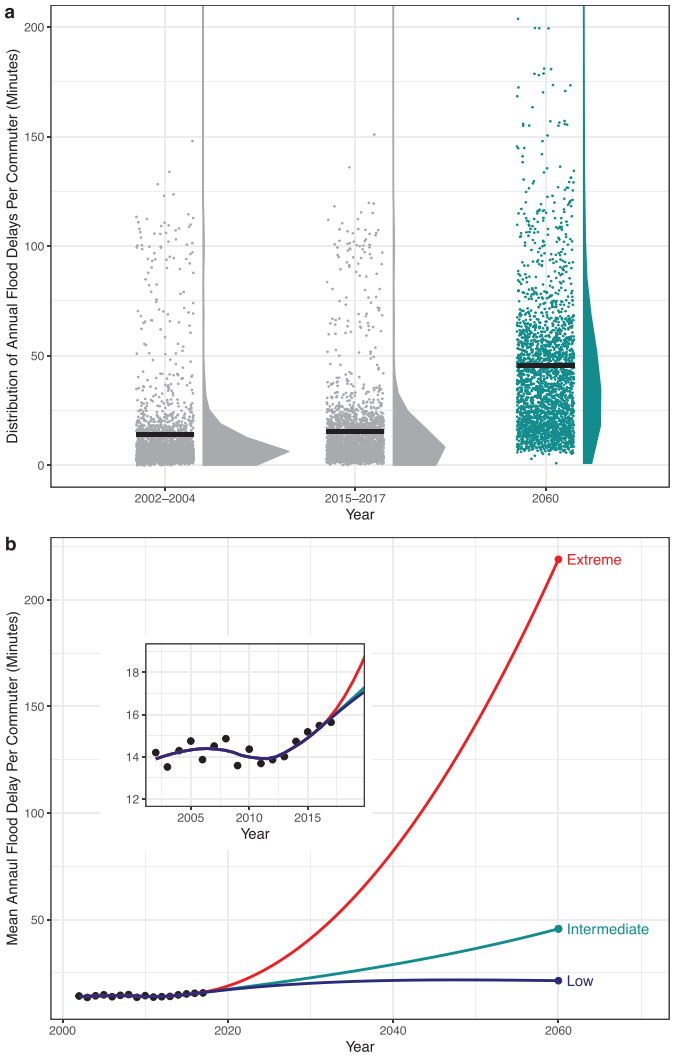

Figure 3. Commuting delays associated with tidal flooding in Miami-Dade and Broward counties. Panel (a) shows the distribution of travel delays due to flooding on roads in each time period. The solid black line indicates the average commuter's flooding delay. The 2060 distribution corresponds to the Intermediate SLR scenario. Dots in panel (b) represent historical average delays for each year from 2002–2018 and anticipated 2060 delays corresponding to tide levels predicted by NOAA low (0.3 m), intermediate (1.0 m), and extreme (2.5 m) 2100 SLR projections assuming 2015–2017 commuter locations. Curves are locally weighted scatterplot smoothing of the respective points. Note that delays before 2018 reflect the influence of SLR, perigean and nodal cycles, and changes in number of commuters on each route.

most heavily impacted (the 'percent impassable commuters' line in table S2) were unable to reach their destination at least once per year due to recurrent tidal flooding in Period 2. In total, approximately 13 700 (95% CI [13 400, 13 800]) people were unable to attend work. Compared to Period 1, the percent of impassable commuters among the entire commuter population increased by 0.26% points, 1.57% points among all impacted commuters, but a decrease of 2.44% points among the most heavily impacted. These results suggest tidal flooding already 'blocks' significant numbers of commuters in the Miami area. The decrease in the percent of impassable commuters amongst the most heavily-impacted areas suggests possible accommodating behavior over time.

Figure 4 illustrates potential accommodation. The number of commuters has grown in those home-work pairs experiencing small increases in travel times while shrinking in home-work pairs with large increases. The figure divides the pairs into 50 min bins based on tidal-flooding induced changes in travel times for a single hypothetical commuter between Periods 1 and 2. Panel (a) shows that only bins with less than a 100 min annual increase in travel time saw a net increase in commuters. Recognizing that changes in absolute numbers of commuters could be driven by a few large home-work pairs, Panel (b) presents the simple average percent change in commuters for each bin. The qualitative results are similar: all bins below 150 min had a significant

Table 1. Tidal flood commuting delays in Miami-Dade and Broward Counties (minutes per commuter per year). Period 1: 2002–2004. Period 2: 2015–2017. Period 3: 2060 (intermediate SLR projections). Assumes road water depth exceeding 30 cm is passable at 1 mph. Displays three sets of home-work Census Block Group centroid pairs: (1) all pairs, (2) pairs experiencing flooding delays in Period 2, and (3) pairs above 95th percentile of flooding delays in Period 2. Change in delays between periods is decomposed into two components: 'Tide effect' is due to changes in road water depth, holding number of commuters in each home-work pair constant at initial period levels; 'Accommodation' is due to changes in number of commuters in each pair, holding water levels constant at final period levels. By construction, total change = tide effect+accommodation.

	(1)		(2)		(3)	
	All home-work pairs		Affected home-work pairs		Top 5% home-work pairs	
	Value	95% CI	Value	95% CI	Value	95% CI
Period 2	15.44	[15.28, 15.59]	103.38	[102.48, 104.29]	274.00	[271.87, 276.13]
Period 2-Period 1	1.43	[1.19, 1.68]	5.99	[4.50, 7.49]	8.21	[4.54, 11.87]
Tide effect	2.03	[1.74, 2.33]	14.16	[12.31, 16.02]	28.57	[23.82, 33.31]
Accommodation	−0.60	[−0.87, −0.33]	−8.17	[−9.79, −6.54]	−20.36	[−24.42, −16.30]
Period 3-Period 2						
Tide effect	30.28	[29.95, 30.61]	155.04	[153.26, 156.81]	140.79	[136.67, 144.91]
Home-work pairs	2817 869		495 182		160 207	
Period 2 commuters	1629 135		242 442		86 154	
Period 1 commuters	1433 163		205 427		73 807	

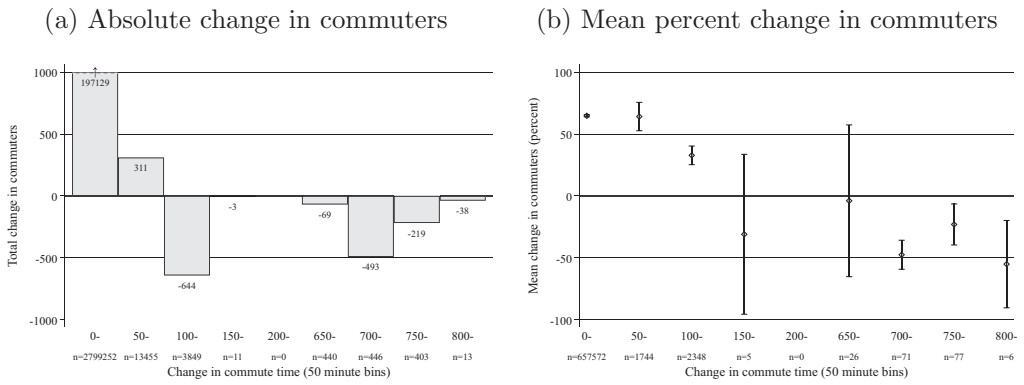

Figure 4. Change in number of commuters travelling between home-work pairs by changes in tidal flooding delays. Both panels divide home-work CBG pairs into bins based on the annual change in travel time attributable to tidal flooding between 2002–2004 and 2015–2017. The number '*n*' indicates how many home-work pairs are in each 50 min bin (there are no home-work pairs in the 200–650 min interval). Panel (a) displays the aggregate net change in commuters for each bin. Panel (b) displays the mean and 95% confidence interval of the percentage change in commuters for those pairs that have at least one commuter in each period.

increase in commuters, while all bins above 700 min had a significant decrease.

These trends are reflected in the accommodation results in table 1. If there were no change in home or work locations from Period 1 levels, travel times would have increased by 2.03 min by Period 2 among the entire commuting population due to increased tidal flooding. The actual increase in commuting time was just 1.43 min, however, suggesting accommodation reduced commuting times by a negligible 0.60 min (36 s) year^{-1}. Accommodation becomes increasingly pronounced amongst pairs with any commuting delays (−8.17 min) and the most heavily impacted areas (−20.36 min). While modest in absolute terms, these changes represent reductions of 29.56%, 57.70%, and 71.23%, relative to no accommodation.

A similar pattern occurs with respect to percent impassable commutes (table S2). The effect of this change in behavior is particularly pronounced for the most exposed category. If home and work locations remained unchanged the percent impassable for this group would have increased by 0.71% points. Changes in behavior, however, reduced the percent impassable by such a large amount (−3.16% points) that the gross percent declined over time despite the increase in tide gauge levels.

Panel (c) of table 1 describes the change in commuting times between Period 2 and Period 3, using intermediate SLR projections. These changes do not account for possible accommodation, holding the number of commuters in each home-work pair constant at Period 2 levels. Panel (b) of figure 3 shows the average annual commuting cost in the historic period and the three SLR projection scenarios in 2060 (Sweet *et al* 2017) holding commuting patterns constant for Period 2. Average commute time for all pairs almost triples from 15.44 to 45.72 min (+30.28 min) and

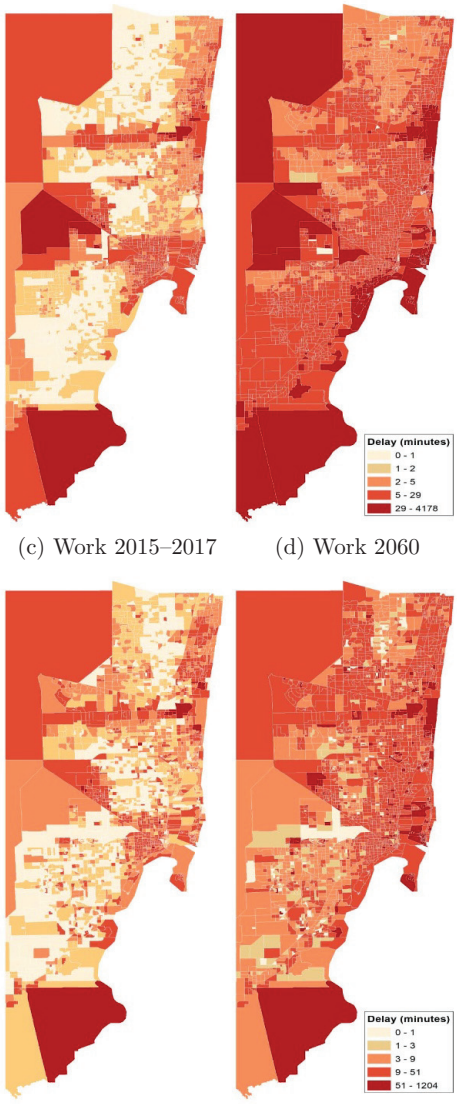

Figure 5. Geographic distribution of average delay per outgoing and incoming commuter. Panels (a) and (b) depict origin (home) CBGs. Panels (c) and (d) depict destination (work) CBGs. Panels (a) and (c) are Period 2. Panels (b) and (d) are Period 3, intermediate SLR scenario. Colors correspond to Period 2 quartiles, with the fourth quartile subdivided into two categories: the 75th–98th percentiles and 99th percentile. Legend assigns the maximum 2060 commuting time as the upper bound for the 99th percentile bins.

could exceed 200 min under the extreme SLR projection. Since this rate of increase is almost twice that of those pairs affected in Period 2, much of the overall increase comes from previously unaffected pairs (table 1). Under the intermediate scenario, among those home-work pairs affected in Period 2, the number of commuters facing at least one impassable trip per year rises from 5.64% to 7.76%, almost the same rate as the top 5% in Period 2 (table S2). With extreme SLR, 3.4% of commuters (about 55 000) may face an impassable trip.

Figure 5 uses equations (4) and (5) to illustrate the geographic distribution of the average delay among all commuters living in a given home CBG (Panels (a) and (b)) and all commuters travelling to a given work CBG (Panels (c) and (d)). Panels (a) and (c) refer to Period 2, while panels (b) and (d) refer to Period 3 intermediate projections. Values are expressed in terms of delays (in mins) per commuter year. In Period 2, the most heavily affected areas for both outgoing and incoming commutes tend to be the corridors radiating northwest from downtown Miami and west from Ft. Lauderdale. There is some variation between home and work impacts, however, with areas to the immediate west and immediate north of Miami experiencing a relatively heavy home impact and areas northwest of Ft. Lauderdale experiencing a relatively heavy work impact. Many of these most affected neighborhoods do not coincide with areas directly affected by flooding, i.e. the actual locations of flooding depicted in blue in figure 2.

Panels (b) and (d) of figure 5 illustrate Period 3 impacts assuming the intermediate NOAA scenario. The majority of CBGs face commuting delays corresponding to the 75th–98th percentile bin in Period 2, between 5 and 29 additional minutes. (Note that percentiles here refer to individual CBGs, while percentiles in table 1 refer to CBG pairs.) Panel (b) shows that by 2060, home CBGs experiencing delays corresponding to the recent period's 99th percentile, greater than 29 min, are prevalent in and around Miami and Ft. Lauderdale, as well as along much of the coast. Panel (d) shows that commuting delays to work CBGs tend to be most pronounced in the area between Miami and Ft. Lauderdale, despite the fact that these areas are expected to have relatively little direct exposure to flooding themselves (figure 2).

The spatial patterns in figure 5 raise the question of the distribution of tidal flooding delays across socioeconomic groups. Figure 6 displays flooding delays for Periods 1 and 2 for each income group, illustrating the decomposition of the change into tidal and accommodation effects (data used to generate the figure are presented in table S3). Panel (a) presents results for all home-work pairs in Miami-Dade and Broward counties. In Period 1, the low-income group has the lowest delays, followed by the high and middle-income groups. This finding is consistent with higher income households living closer to the coastal areas most likely to experience tidal flooding. Keeping commuting patterns fixed at Period 1, but using Period 2 tidal gauge data indicates the tidal effect on commuting delays. The figure shows that all three groups experience almost the same increase in commuting times due to rising tide gauge readings. Keeping tide gauges at Period 2 levels, but allowing commuting patterns to change from Period 1 to Period 2 illustrates accommodation. While all

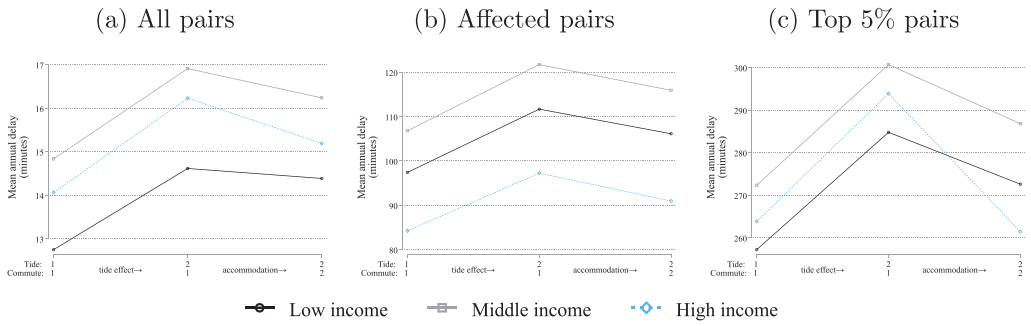

Figure 6. Tide and accommodation effects on commuting delays over time by commuter income. Period 1: 2002–2004. Period 2: 2015–2017. Low income: <$1250 per month. Middle income: $1251–$3333 per month. High income: >$3333 per month. The *x* axis indicates combinations of tidal and commuter data, by period. Tide effect represents the impact of changes in tide gauge readings from Period 1 to Period 2, holding commuting patterns fixed in Period 1. Accommodation effect represents the impact of changes in commuting patterns from Period 1 to Period 2, holding tide gauge readings fixed in Period 2.

three income groups demonstrate a tendency to shift their home or work locations in a way that moderates the change in commuting delays, this effect appears pronounced among the high-income group.

Panel (b) restricts attention to only those home-work CBG pairs that experienced some flooding delays in Period 2. It only shows the reallocation of commuters within the set of affected pairs. It thus does not capture the effect of commuters switching to unaffected home-work pairs. Among affected pairs, the highest income group has the lowest average delay in Period 1. As in Panel (a) the tidal effect is parallel across the three groups. Although the highest income group shows the largest accommodation effect, the difference with the other groups is less pronounced than in Panel (a).

Panel (c) further focuses on only the 5% of home-work pairs most highly impacted by flooding delays in Period 2. In this group, as in Panel (a), low-income commuters are the least affected, followed by high and middle income. Here, the differences in accommodation are striking. Changes in location among all three groups appear to have moderated the average flooding delay. While there does not seem to be much difference in accommodation among low and middle income commuters, location changes for the high income group were such that Period 2 delays were *lower* than Period 1 delays despite the higher tide levels. It is important to emphasize, however, that as before the accommodation results are descriptive and do not have a causal interpretation. When analyzing income groups we have the additional challenge that we cannot identify changes in average group commuting time arising from other factors. Changes in wages over time, for example, may cause commuters to shift from one income group to another, affecting mean commuting time without any change in location.

4. Discussion

While overall commuting times have risen due to road inundation, changes in home and/or work locations since 2002 have ameliorated this impact, particularly among the highest income commuters. Such potential accommodation should not be ignored when planning future infrastructure investments and adaptation policies. In locations facing increasing burdens on travel to work (the top 5th percentile), the relocation of commuter residential and work locations over time offset the costs net of adaptation by over 70%. Private accommodation potentially undermines the benefits of investments aimed to protect coastal residents.

To maintain tractability, our model makes several simplifying assumptions commonly employed in the literature. Spatial variation in surface water depth uses a bathtub model under an assumption of perfect hydraulic connectivity similar to NOAA. In general, the areas our model predicts to be flooded during high tides, as visualized in figure 2, closely resemble the high tide predictions of NOAA's Sea Level Rise Viewer (2020). Lacking data on placement, implementation, and effectiveness of road pumps, sea walls, raised streets, backflow preventers, etc our model ignores possible impacts of such adaptive infrastructure. Taken together these assumptions could lead our model to overstate the incidence of tidal flooding. However, due to the porous limestone geography, subsurface flows play a significant role in nuisance flooding in the Miami area, potentially limiting the bias of these assumptions.

Other factors in the model may lead to understating the flooding impacts. Apart from the direct impact on street flooding, high tides adversely affect drainage. Since our model implicitly assumes no rainfall, it does not include street flooding caused by the combination of precipitation and high tides.

Regarding driver behavior, the model does not account for possible street congestion, which may further increase commuting times during flood events as commuters redirect to fewer streets.

In addition to improving the precision of flooding measurement, future research could benefit from expanding the geographic scope and the population of commuters investigated. For example, we only evaluate commutes between CBGs. Data limitations prevent us from estimating commuting delays for people living and working within the same CBG—potentially underestimating impacts for workers living in CBGs susceptible to tidal flooding. We also omit impacts for those commuting between Miami-Dade or Broward and other surrounding counties. The additional commuting time imposed by tidal flooding may push long-distance travelers to migrate if their tolerance threshold for commuting is exceeded. Finally, cities with high levels of public transportation may observe distinct accommodation patterns (Kasmalkar *et al* 2020). Thus, replicating this analysis in other cities will be crucial to informing urban adaptation policies.

Understanding the limitations of private accommodation is of utmost importance to inform policy decisions. Our preliminary analysis indicates that commuters in the middle-income wealth category ($1251–$3333 per month) are hardest hit by commuting delays. The high-income category (more than $3333 per month) has the greatest potential to avert delays through accommodation. We interpret these results qualitatively because our approach is unable to control for auxiliary factors that would influence the findings, such as changes in wages over time. Approximating these heterogeneous effects, however, should not be taken lightly going forward, as identifying the appropriate city investment, whether it be building a sea wall or expanding social protection, will depend on the beneficiaries being targeted.

Data availability statement

The data that support the findings of this study are available upon reasonable request from the authors.

ORCID iDs

Valerie Mueller https://orcid.org/0000-0003-1246-2141
Glenn Sheriff https://orcid.org/0000-0001-9642-5529

References

Adger W N, Lorenzoni I and O'Brien K L 2009 *Adapting to Climate Change: Thresholds, Values, Governance* (Cambridge: Cambridge University Press)
Bakkensen L, Ding X and Ma L 2019 Flood risk and salience: new evidence from the sunshine state *South. Econ. J.* **85** 1132–58
Bernstein A, Gustafson M and Lewis R 2019 Disaster on the horizon: the price effect of sea level rise *J. Financ. Econ.* **5** 253–72
Bin O and Landry C 2013 Changes in implicit flood risk premiums: empirical evidence from the housing market *J. Environ. Econ. Manage.* **65** 361–76
Bukvic A and Harrald J 2019 Rural versus urban perspective on coastal flooding: the insights from the U.S. Mid-Atlantic communities *Clim. Risk Manage.* **23** 7–18
Carbone J, Hallstrom D and Smith V 2006 Can natural experiments measure behavioral responses to environmental risks? *Environ. Resour. Econ.* **33** 273–97
Chamberlain S 2019 rnoaa: 'NOAA' weather data from R. R package version 0.9.0 (available at: https://CRAN.R-project.org/package=rnoaa)
Chen C and Liu L-M 1993 Forecasting time series with outliers *J. Forecast.* **12** 13–35
Clark P *et al* 2016 Consequences of twenty-first-century policy for multi-millennial climate and sea-level change *Nat. Clim. Change* **6** 360–9
Dahl K, Fitzpatrick M and Spanger-Siegfried E 2017 Sea level rise drives increased tidal flooding frequency at tide gauges along the US east and gulf coasts: projections for 2030 and 2045 *PLoS One* **12** e0170949
de Lacalle J L 2019 tsoutliers: detection of outliers in time series. R package version 0.6-8 (available at: https://CRAN.R-project.org/package=tsoutliers)
Deryugina T, Kawano L and Levitt S 2018 The economic impact of Hurricane Katrina on its victims: evidence from individual tax returns *Am. Econ. J.: Appl. Econ.* **10** 202–33
Desmet K, Kopp R, Kulp S, Nagy D, Oppenheimer M, Ross-Hansberg E and Strauss B 2021 Evaluating the economic cost of coastal flooding *Am. Econ. J.: Macroecon.* **13** 444–86
Dronkers J *et al* 1990 *Strategies for Adaptation to Sea Level Rise: Report of the IPCC Coastal Zone Management Subgroup* (Geneva: Intergovernmental Panel on Climate Change)
Florida Department of Transportation 2020a Speed zoning for Florida (available at: www.fdot.gov/traffic/speedzone/speed-zone-manual.shtm) (Accessed 1 February 2020)
Florida Department of Transportation 2020b Transportation and data analytics, geographic information system (available at: www.fdot.gov/statistics/gis/default.shtm#Traffic) (Accessed 1 February 2020)
Florida R and Pedigo S 2019 Stuck in traffic: for greater Miami to become a leading startup hub, better mobility is a must *Technical Report* (Florida International University)
Garner A, Mann M, Emanuel K, Kopp R, Lin N, Alley R, Horton B, DeConto J and Pollard D 2017 Impact of climate change on New York City's coastal flood hazard: increasing flood heights from preindustrial to 2300 CE *Proc. Natl Acad. Sci.* **114** 11861–6
Gesch D, Oimoen M, Greenlee S, Nelson C, Steuck M and Tyler D 2002 The national elevation dataset *Photogramm. Eng. Remote Sens.* **68** 5–32
Hallegatte S, Ranger N, Mestre O, Dumas P, Corfee-Morlot J, Herweijer C and Wood R 2011 Assessing climate change impacts, sea level rise and storm surge risk in port cities: a case study on Copenhagen *Clim. Change* **104** 113–37
Hauer M E 2017 Migration induced by sea-level rise could reshape the U.S. population landscape *Nat. Clim. Change* **7** 321–5
Hauer M, Evans J and Mishra D 2016 Millions projected to be at risk from sea-level rise in the continental United States *Nat. Clim. Change* **6** 691–5
Hinkel J *et al* 2014 Coastal flood damage and adaptation costs under 21st century sea-level rise *Proc. Natl Acad. Sci.* **111** 3292–7
Hino M, Belanger S, Field C, Davies A and Mach K 2019 High-tide flooding disrupts local economic activity *Sci. Adv.* **5** eaau2736
Hsiang S and Kopp R 2018 An economist's guide to climate change science *J. Econ. Perspect.* **32** 3–32

Jacobs J M, Cattaneo L R, Sweet W and Mansfield T 2018 Recent and future outlooks for nuisance flooding impacts on roadways on the U.S. East Coast *Transp. Res. Rec.* **2672** 1–10

Kasmalkar I G, Serafin K A, Miao Y, Bick I A, Ortolano L, Ouyang D and Suckale J 2020 When floods hit the road: resilience to flood-related traffic disruption in the San Francisco bay area and beyond *Sci. Adv.* **6** eaba2423

Kocornik-Mina A, McDermott T K, Michaels G and Rauch F 2020 Flooded cities *Am. Econ. J.: Appl. Econ.* **12** 35–66

Kopp R, Gilmore E, Little C, Lorenzo-Trueba J, Ramenzoni V and Sweet W 2019 Usable science for managing the risks of sea-level rise *Earth's Future* **7** 1235–69

Kulp S and Strauss B 2017 Rapid escalation of coastal flood exposure in US municipalities from sea-level rise *Clim. Change* **142** 477–89

McAlpine S and Porter J 2018 Estimating recent local impacts of sea-level rise on current real-estate losses: a housing market case study in Miami-Dade, Florida *Popul. Res. Policy Rev.* **37** 871–95

Miami-Dade County 2020 Miami-Dade county open data hub *Street Maintenance* (available at: gis-mdc.opendata.arcgis.com/datasets/street-maintenance) (Accessed 1 February 2020)

Michael J 2007 Episodic flooding and the cost of sea-level rise *Ecol. Econ.* **63** 149–59

Moftakhari H, AghaKouchak A, Sanders B, Feldman D, Sweet W, Matthew R and Luke A 2015 Increased nuisance flooding along the coasts of the United States due to sea level rise: past and future *Geophys. Res. Lett.* **42** 9846–52

Moftakhari H, AghaKouchak A, Sanders B and Matthew R 2017 Cumulative hazard: the case of nuisance flooding *Earth's Future* **5** 214–23

NOAA 2017 *Detailed Method for Mapping Sea Level Rise Inundation* (Office for Coastal Management)

NOAA 2020 Sea level rise viewer tool's high tide flooding (available at: https://coast.noaa.gov/digitalcoast/tools/slr.html) (Accessed 13 November 2020)

Praharaj S, Chen T, Zahura F, Behl M and Goodall J 2021 Estimating impacts of recurring flooding on roadway networks: a Norfolk, Virginia case study *Nat. Hazards* 1–25

Pregnolato M, Ford A, Wilkinson S M and Dawson R J 2017 The impact of flooding on road transport: a depth-disruption function *Transp. Res.* D **55** 67–81

Sadler J, Haselden N, Mellon K, Hackel A, Son V, Mayfield J, Blase A and Goodall J 2017 Impact of sea-level rise on roadway flooding in the Hamptom Roads region, Virginia *J. Infrastruct. Syst.* **23**

Shen S and Kim K 2020 Assessment of transportation system vulnerabilities to tidal flooding in Honolulu, Hawaii *Transp. Res. Rec.* **2674** 207–19

Suarez P, Anderson W, Mahal V and Lakshmanan T 2005 Impacts of flooding and climate on urban transportation: a systemwide performance assessment of the Boston Metro Area *Transp. Res.* D **10** 231–44

Sweet W V, Dusek G, Obeysekera J and Marra J J 2018 Patterns and projections of high tide flooding along the U.S. coastline using a common impact threshold *Technical Report* NOS CO-OPS 086 (NOAA)

Sweet W V, Kopp R E, Weaver C P, Obeysekera J, Horton R M, Thieler E R and Zervas C 2017 Global and regional sea level rise scenarios for the United States *Technical Report* NOS CO-OPS 083 (NOAA)

U.S. Census Bureau 2020a 2019 tiger/line shapefiles (available at: www.census.gov/cgi-bin/geo/shapefiles/index.php?year=2019&layergroup=Roads)

U.S. Census Bureau 2020b LEHD origin-destination employment statistics (2002–2017) *Longitudinal-Employer Household Dynamics Program* (LODES 7.4.) (available at: onthemap.ces.census.gov) (Accessed 1 February 2020)

Yi D and Choi H 2019 Housing market response to new flood risk information and the impact on poor tenant *J. Real Estate Finance Econ.* **5** 1–25